Available online at www.sciencedirect.com
ScienceDirect
Tetrahedron
Tetrahedron 63 (2007) 7457–7467

Effect of ionic strength on the self-assembly, morphology and gelation of pH responsive β-sheet tape-forming peptides

Lisa M. Carrick,[a] Amalia Aggeli,[a,*] Neville Boden,[a] John Fisher,[b] Eileen Ingham[b] and Thomas A. Waigh[c,†]

[a]*Centre for Self-Organising Molecular Systems, Department of Chemistry, University of Leeds, Leeds, West Yorkshire LS2 9JT, UK*
[b]*Institute of Medical and Biological Engineering, School of Mechanical Engineering, University of Leeds, Leeds, West Yorkshire LS2 9JT, UK*
[c]*School of Physics and Astronomy, University of Leeds, Leeds, West Yorkshire LS2 9JT, UK*

Received 13 December 2006; revised 3 May 2007; accepted 8 May 2007
Available online 13 May 2007

Abstract—Molecular self-assembly is an intrinsic property of proteins central to their biological functionality. One important industrially interesting property is the ability to control and switch on and off self-assembly using a variety of external chemical and physical triggers. Model peptides have been developed with significantly reduced chemical and structural complexity compared to biological proteins. These are ideal systems for exposing the fundamental principles that drive protein-like self-assembly, as well as for establishing in a quantitative manner their structure–function relationship. We investigate simple, short model peptides that adopt a purely β-strand conformation, align in an antiparallel manner and self-assemble in one dimension in solution into long β-sheet nanotapes and higher order aggregates with no other conformation (i.e., helices, turns or random coils) present in the aggregates. These micrometre-long nanostructures gel in solutions at concentrations as low as 0.2% v/v. Their gel–fluid transition has been previously shown to be controlled by pH, temperature, or by mixing with complementary peptides. Here we show the dramatic effect of another chemical trigger, that of physiological-like salt concentration, on the self-assembly, morphology and gelation of a series of systematically designed charged self-assembling tape-forming peptides, each 11 amino acid residues in length, in the pH range of 2–14. This study provides a detailed understanding of the self-assembly of this class of peptides in aqueous solutions of biologically relevant pH and ionic strength. This insight has led to the development of injectable self-assembling peptide lubricants as potential therapeutics for the treatment of early stage knee joint osteoarthritis.

1. Introduction

Protein-like self-assembly has been the focus of intense research over the last years, due to its importance for understanding amyloid diseases, as well as due to applications in the emerging field of nanotechnology.[1–12] In our laboratory, we have previously developed one of the simplest model peptide systems which, above a critical concentration (c^*) in solution, undergoes nucleated one-dimensional self-assembly into well-defined twisted micrometre-long β-sheet aggregates, such as helical tapes, twisted ribbons, fibrils and fibres as a function of peptide concentration.[13–20] At higher concentrations (typically higher than 0.2 wt %), these long supramolecular structures can give rise to isotropic or nematic organogels and hydrogels. A theoretical model has been developed, which can quantitatively describe peptide self-assembly in terms of a set of molecular energetic parameters.[21,22] This hierarchical self-assembly behaviour has been shown to stem from the chirality of the individual peptide molecules, which gives rise to an intrinsic twist about the tape long axes: left handed in the case of peptides made of L-amino acids.[23] The finite fibril width and helicity has its origin in the competition between the free energy gain from attraction between ribbons and the free energy cost of elastic distortion of the intrinsically twisted ribbons on incorporation into a growing fibril. This hierarchical self-assembling behaviour also provides an explanation for the structure and stability of amyloid fibrils formed by more complex proteins in vivo. The well-defined self-assembled structures have been used as templates for nanostructured inorganic materials such as hollow silica nanotubes,[24] nucleation of biominerals[25] and surface nanocoatings.[26]

The ability of these peptides to self-assemble into β-sheet tapes and stack to form fibrils can be utilised to establish model systems in which the systematic exchange of individual amino acids within the peptide primary structure can be studied. For example, the incorporation of ionisable side chains into the sequence allows the introduction of pH

* Corresponding author. E-mail: a.aggeli@leeds.ac.uk
† Present address: Biological Physics, School of Physics and Astronomy, University of Manchester, PO Box 88, Sackville St., Manchester M60 1QD, UK.

0040–4020/$ - see front matter © 2007 Elsevier Ltd. All rights reserved.
doi:10.1016/j.tet.2007.05.036

responsiveness into the system, where in the absence of charged side chains there was none.[27,28] It can be determined how, on a simple level, exchanging acidic for basic side chains, and vice versa, changes the macromolecular state, i.e., gel or fluid of the solutions at fixed pH values. At a more detailed level, it can be identified that the change in physical state of the solutions is as a result of the electrostatic repulsive or attractive interactions between neighbouring charged groups on the peptide molecules.

Likewise, the effect of exchanging larger hydrophilic glutamine side chains ($-(CH_2)_2CONH_2$) for smaller, more hydrophilic serine side chains ($-CH_2OH$) can be studied. The interactions between amino acid residues within a fibril, and also between amino acids and the surrounding solvent are important in producing stable, soluble fibrils, and the effect of the reduction in the size of the side chain on the molecular packing of peptides within the fibrillar structure can be observed.

The control exerted by electrostatic interactions naturally leads to the question of how the self-assembly would be affected by changing the ionic strength in solution. An increase in salt concentration in water would be expected to shield the electrostatic forces and shift both the critical concentration required for the onset of self-assembly and the observed pH of the transition from gel to fluid. The influence of biologically relevant ionic strength on the self-assembly and gelation of systematically varied β-sheet tape-forming peptides was the purpose of the current investigation.

The primary structures of these peptides are given in Table 1. The amino acid side chains that contain an ionisable acid group are indicated by a negative charge while those that contain ionisable basic groups are indicated by a positive charge. The distribution of electrical charges on each peptide will depend on the pH in solution.

Table 1. Peptide primary structures: amino acid residues are numbered 1 to 11 from the N- to the C-terminal (left to right); O: ornithine

Peptide	Primary structure
P_{11}-4	CH_3CO-Q^1-Q-R^+-F-E^--W-E^--F-E^--Q-Q^{11}-NH_2
P_{11}-8	CH_3CO-Q-Q-R^+-F-O^+-W-O^+-F-E^--Q-Q-NH_2
P_{11}-9	CH_3CO-S-S-R^+-F-E^--W-E^--F-E^--S-S-NH_2
P_{11}-12	CH_3CO-S-S-R^+-F-O^+-W-O^+-F-E^--S-S-NH_2

2. Results and discussion

Peptide P_{11}-4 was designed to form β-sheet fibrils and gels at low pH and to convert to a monomeric fluid solution at high pH, in all cases in pure water in the absence of any added salt.[27] The material change is driven by the deprotonation of the glutamic acid ($-CH_2CH_2COOH$) side chains in positions 5, 7 and 9 and is shown to correspond to a change in peptide secondary structure from β-sheet to random coil.

The self-assembly behaviour of P_{11}-4 was studied at c=6.3 mM (equivalent to ca. 0.7% v/v) at pH 1–14. Band fitting of FTIR absorption spectra was used as a semi-quantitative method for the determination of the proportion of peptide in β-sheet aggregates as a function of pD. In order to further verify and to increase the accuracy of the β-sheet content determination, FTIR data were combined with solution ^{1}H NMR data.

In the absence of any added salt, at pD<~3, P_{11}-4 forms self-supporting cloudy gels (Fig. 1a). FTIR reveals a large absorption band centred at 1618 cm^{-1} corresponding to peptide in a β-sheet conformation, with the weak band at 1682 cm^{-1} indicating an antiparallel arrangement (Fig. 1c(i)). The high resolution ^{1}H NMR spectrum (Fig. 1d(i)) shows a structureless, broad banded trace, indicative of peptide molecules locked into a relatively static fibril. In this pH range the peptide has a net +1 charge from the charge on the Arg3 side chain.

At pD>3.4, milky flocculates are obtained, composed of insoluble self-assembled aggregates. The insolubility is due to the electrical charge neutrality on each peptide molecule. The charged arginine ($-(CH_2)_3CNH(NH_2)C{=}NH$) side chain in position 3 is balanced by the negative charge of the glutamic acid in position 9.

As the pD is increased further other glutamic acid side chains in the peptide molecule become increasingly deprotonated, and viscous weakly nematic fluids are observed, due to the net negative charge on the peptide. As the pH increases further, more glutamic acid side chains in the peptide become deprotonated, the net peptide charge increases and the repulsion between peptides in fibrils and fibres increases still further giving a higher proportion of peptide molecules in a monomeric state. FTIR (Fig. 1c(ii)) spectra indicate a reduced β-sheet absorption band at 1618 cm^{-1} matched in intensity by a band at 1645 cm^{-1} corresponding to peptide in a random coil state, which increases in magnitude as a function of pD.

The deprotonation of the glutamic acid side chains as a function of pH can be monitored by FTIR. At pD≤4 a weak absorption band is observed at 1710 cm^{-1}, which has been assigned to COOD of protonated glutamic acid side chains. At pD≥4 an absorption band in the amide II′ region at 1565 cm^{-1} is observed, which is assigned to COO^- of deprotonated glutamic acid side chains. This band is seen to increase with intensity as the pD of the solution is increased from 4 to 8.

At pD 8–9 the β-sheet aggregates completely disintegrate into monomeric peptide (Fig. 1a and c). In the pH range 9–12, all glutamic acid side chains are deprotonated and the net peptide charge becomes −2. At pH>12, the Arg3 side chain also loses its proton, and the net peptide charge becomes −3. The high resolution ^{1}H NMR spectrum of a solution of P_{11}-4 at pD 12 (Fig. 1d(ii)) consists of sharp peaks corresponding to peptide protons, indicative of monomeric peptide molecules undergoing fast random, reorientational motion. To confirm that solutions at pD>10 contain only monomeric peptide, we observe that for a 6.3 mM solution the magnitude of the intensity of the NMR band is ~10 times that observed for a 0.6 mM solution (unpublished data, data not shown). This direct relationship between band intensity and peptide concentration indicates that these basic solutions contain no β-sheet. Additionally, titrating the solutions to even higher pD solutions gave no further increase in the band intensity, showing that

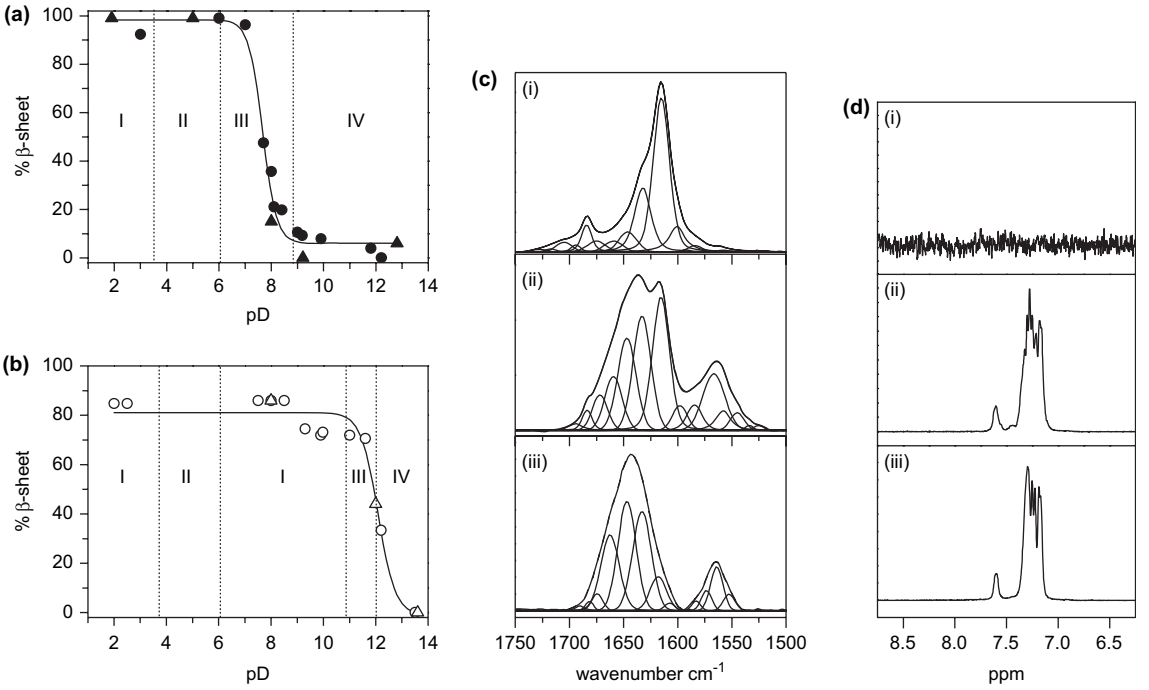

Figure 1. Self-assembly of P_{11}-4 at c=6.3 mM. (a) Percentage β-sheet of P_{11}-4 as determined by FTIR (●) and solution ^{1}H NMR (▲) as a function of pD in D_2O with no added salt. (b) Percentage β-sheet of P_{11}-4 as determined by FTIR (○) and NMR (△) as a function of pD in 130 mM NaCl in D_2O (note that the solid lines are to guide the eye and do not represent a best fit): I: nematic gel, II: flocculate, III: nematic fluid, IV: isotropic fluid. (c) FTIR absorption spectra of P_{11}-4 in D_2O showing (i) nematic gel at pD 2, (ii) viscous nematic fluid at pD 7.7, (iii) isotropic solution at pD 11.8. (d) ^{1}H NMR spectra of P_{11}-4: (i) broad banded spectrum corresponding to aggregated peptides in a nematic gel at pD 2 in D_2O, (ii) aromatic protons of monomeric peptide in a clear isotropic fluid at pD 12 in D_2O and (iii) in clear isotropic fluid at pD 13.5 in 130 mM NaCl.

all peptide is in the monomeric state by pD 9. The critical concentration required for the onset of peptide self-assembly is dependent on the ionisation state of the amino acid side chains. The concentration at which P_{11}-4 self-assembly occurs therefore increases as the pH/pD of the solution increases.

The transition from β-sheet to random coil is particularly sharp in the absence of added salt and occurs over the range of pD 7.5–8. The sharpness of this transition is driven by the increase in negatively charged glutamic acid side chains. To investigate the balance between the degree of charge and the structural transition, the effect of increasing the ionic strength was studied. In order for this study to be relevant to biological-like conditions, aqueous solutions with 130 mM added NaCl were studied here, similar to the concentration of NaCl in the blood. It is expected that as the ionic strength in solution is increased, the electrostatic repulsion between Glu^- would be decreased due to the shielding of charge by salt counterions.

It was found that increasing the ionic strength of the solution by the addition of 130 mM NaCl shifts the transition to monomer to higher pD values by more than 4 units (Fig. 1b). Preliminary titration experiments of solutions of P_{11}-4 also suggest that there is no apparent effect of ionic strength on the deprotonation of glutamic acid side chains as a function of pH (data not shown). This implies that the observed effect of ionic strength on the pH responsiveness of the peptide gels is mainly due to screening of electrostatic repulsions rather than change of the deprotonation behaviour of the glutamic acid side chains and of the net peptide charge as a function of pH. Another effect of added salt is that the nematic gel (region I in Fig. 1b) now extends over two pD regions: 6–11 and 2–3.8. In contrast, at this peptide concentration in the absence of salt, nematic gels were only obtained in the pD range of 2–3.4.

The gels in D_2O in the absence of added salt (region I) are shown by electron microscopy to be composed of fibrils and fibres, which are micrometres in length. Typically fibrils are observed with widths in the range 12–19 nm at their widest point, and 9–13 nm at their thinnest point. They exhibit a helical pitch of 200–426 nm. A typical fibril has a width equal to 15 nm (Fig. 2c) and narrows to 9 nm with a helical pitch of 225±10 nm. Figure 2a shows the association of two fibrils, each with width equal to 13 nm coiling together to form a large fibre 23 nm in width. Such entanglements may provide evidence of the nature of gelation through fibre formation. Flocculates and nematic fluids (regions II and III in Fig. 1a) are also shown to be composed of similar fibrils and fibres.

Some fibrils can be seen to dissociate into thinner self-assembled structures, ~4 nm in width. These 4 nm wide ribbons or fibrils are only observed in these cases, rather than as a separate population. Occasionally rings 5–40 nm in diameter are observed along with small amorphous aggregates or 'nanoparticles' but these are relatively few in number in comparison to fibrils and fibres.

Despite the dramatic shift in the pD at which the transition from β-sheet to monomer occurs on moving from low salt to high salt solution, the most frequently observed fibrillar

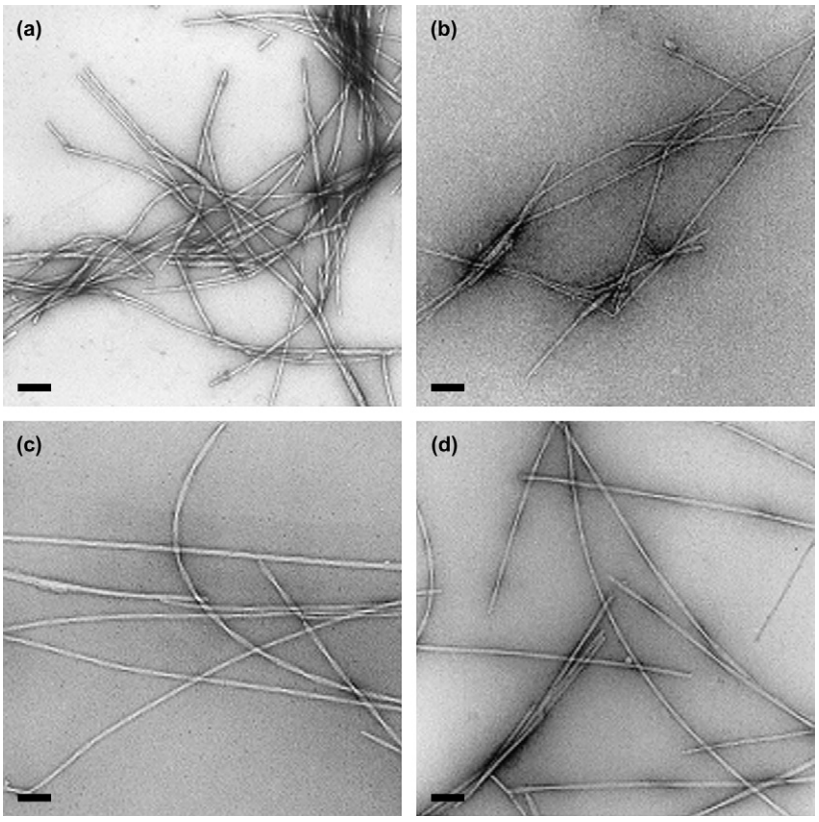

Figure 2. TEM micrographs of P_{11}-4 solutions with c=6.3 mM: (a) nematic gel at pD 3 in D_2O, (b) flocculate at pD 6 in D_2O, (c) nematic gel of P_{11}-4 at pD 9.3 in 130 mM NaCl, (d) viscous fluid at pD 11.6 in 130 mM NaCl. Scale bars correspond to100 nm.

morphologies appear to be independent of ionic strength and pD over the pD range 1–8.5 in D_2O, and 1–11 in 130 mM NaCl.

It has also been observed that converting the gel to monomer by heating to temperature >70 °C or switching the pH will allow the reassembly and gelation of peptides on cooling to room temperature or at an appropriate pH. The pH behaviour has been shown to be reversible by titrating solutions up to six times.

Peptide P_{11}-8 was designed to display the converse pH switching behaviour to P_{11}-4. P_{11}-8 was expected to be in the monomeric state at low pH in solution, and to form fibrillar aggregates at high pH. This opposite behaviour is driven by the incorporation of basic amino acids rather than acidic amino acids into the peptide primary structure (Table 1). P_{11}-8 has an arginine side chain at position 3, ornithine ($-(CH_2)_3NH_2$) side chains at positions 5 and 7 and a glutamic acid side chain at position 9. The side chains of free arginine and free ornithine are positively charged in solution below their pK_a values of 12.5 and 10.8, respectively.

At pD<6 in D_2O P_{11}-8 forms clear isotropic fluids at a peptide concentration of 6.4 mM. FTIR spectra (Fig. 3c(i)) show a broad absorption band at 1645 cm^{-1}, which is assigned to peptides in the random coil state. The band at 1672 cm^{-1} is residual TFA^- from the peptide cleavage and purification. The behaviour at pD<6 is due to the +2 net charge per peptide (+3 at pD<4). At 6<pD≤10.3 biphasic solutions containing gel particles dispersed in a clear fluid are observed. The proportion of gel to fluid within this mixture increases as the pD approaches 10.3. Optical microscopy reveals that the gel particles are nematic whilst the fluid is isotropic (data not shown). FTIR reveals a large absorption band centred at 1614 cm^{-1} corresponding to peptide in a β-sheet conformation, with the weak band at 1684 cm^{-1} indicating an antiparallel arrangement. At 6<pD≤10.3 the ornithine side chains become progressively deprotonated, thus gradually decreasing the net charge per peptide and also the intermolecular electrostatic repulsion, thus allowing self-assembly to take place.

At pD≥10.3±0.3, nematic gels are observed, which are shown by FTIR to have a characteristic β-sheet absorption band at 1614 cm^{-1}. Figure 3c(ii) shows the FTIR spectrum of P_{11}-8 at pD 12.8. It is interesting to note that gels formed at pD≥13 are weaker than those observed at pD 10–13. This applies to gels in D_2O (no added salt) as well as those with increased ionic strength (130 mM NaCl). This may be explained if we consider the electric charges on the amino acid side chains. The ornithine side chains would be expected to achieve their fully deprotonated state at pD>∼11 ($-(CH_2)_3NH_2$), so the only charged groups would be Arg^+ and Glu^-. This means that the net electronic charge per peptide would be 0 and the fibrils would be expected to flocculate out of solution at pD>11. However, reaction of CO_2 with the amino groups on deprotonated Orn at high pH leads to formation of carbamate (RNHCOO–) groups.[27–29] Repulsion from these negatively charged carbamates would be enough to stabilise the fibrillar dispersion and to give rise to gels. At pD>13 the arginine side chain will also be

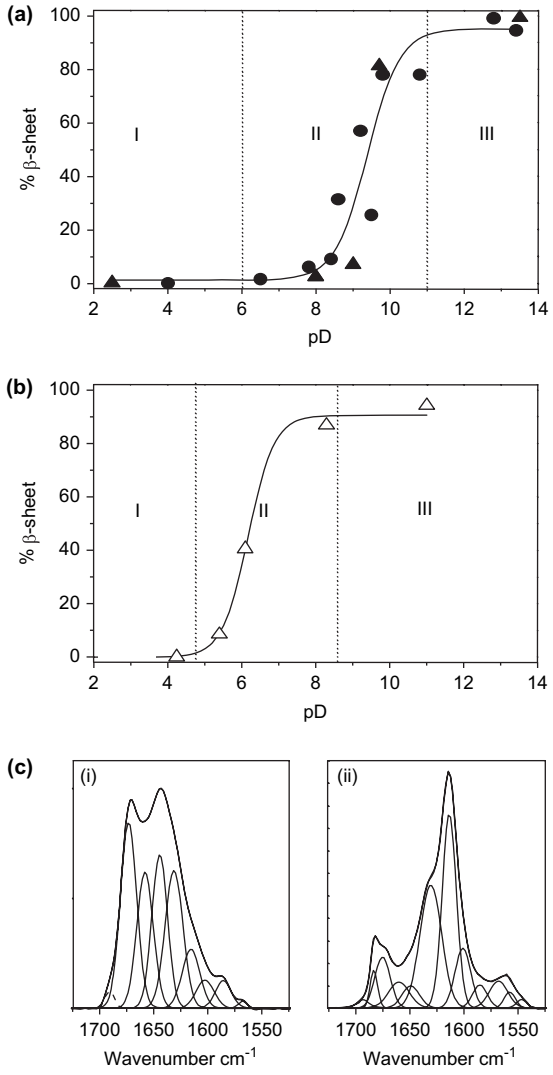

Figure 3. (a) Percentage β-sheet of P_{11}-8 as determined by FTIR (●) and NMR (▲) as a function of pD in D_2O. (b) Percentage β-sheet of P_{11}-8 as determined by NMR (△) as a function of pD in 130 mM NaCl in D_2O: I: isotropic fluid, II: biphasic solution, III: nematic gel. (c) FTIR absorption spectra of P_{11}-8 (c=6.4 mM) in D_2O showing (i) monomer at pD 4, (ii) strong self-supporting β-sheet gel at pD 12.8.

deprotonated, so that there will be an even higher number of net negative charges per molecule coming from the glutamic acid and the carbamate side chains. This high net negative charge may be destabilising the process of self-assembly and lead to the weaker gels.

The analysis of the FTIR data for P_{11}-8 (shown in Fig. 3a) is more scattered than that observed for P_{11}-4 (Fig. 1a). This is because of the difficulty of collecting the data. Biphasic solutions and gels readily separate upon the application of 'mechanical force' or compression between CaF_2 discs when sampling occurs for FTIR. This leads to disproportionate amounts of gel and fluid between the IR discs and leads to inaccurate determination of β-sheet content. ^{1}H NMR reveals that the transition occurs at a similar pD value to that observed using FTIR (Fig. 3a).

It has been shown that P_{11}-8 does indeed self-assemble into β-sheet fibrils at high pH values and forms monomeric peptide solutions at low pH. The pH-dependent behaviour of P_{11}-8 is not exactly the converse of P_{11}-4. This can be seen by comparing their phase behaviours (Fig. 1a and b and Fig. 3a and b). P_{11}-4 forms viscous nematic fluids in the region of the transition between gel and fluid ($8.5>pD\geq7$), whereas in the transition region for P_{11}-8 ($6\leq pD<11$) we observe biphasic solutions. These two physically different states have been shown to have approximately the same percentage β-sheet. In addition the physical properties of the two gel states are also different. P_{11}-4 gels are shear softening, i.e., if sheared they will flow but after some time, they will return to their original gel state. If a P_{11}-8 gel is sheared it will break into gel particles and give rise to a biphasic solution. The bulk gel state will not reform with time. As was observed for P_{11}-4, the pH switching behaviour of P_{11}-8 is reversible. The gel can also be converted to fluid solution by heating to temperatures >80 °C and will reform on cooling.

Upon addition of 130 mM NaCl, the random coil to β-sheet transition is seen to shift by 3 pH units to lower pH (Fig. 3b). P_{11}-8 solutions were observed to contain gel particles at $4.4\leq pD\leq8.5$, whilst at $pD\geq8.5$ self-supporting gels were observed.

At $pD\geq8$ in D_2O, P_{11}-8 is observed by electron microscopy to self-assemble into fibrils and fibres of similar dimensions over the whole range $8\leq pD\leq13.5$. Fibrils with typical widths in the region of 7–14 nm and several μm in length are observed (Fig. 4). In some cases fibres 20–30 nm in width can be seen that are comprised of a number of 8–14 nm wide fibrils stacked (coiled) together into a rope-like structure. In fact, the most striking difference between P_{11}-4 and P_{11}-8 fibrils is this tendency for the P_{11}-8 fibrils to be loosely associated allowing the composition of the fibres to be ascertained. P_{11}-4 fibres are more tightly packed, and may in fact be comprised of fewer fibrils, which are more highly twisted.

The only pH-dependent behaviour of the P_{11}-8 self-assembled aggregates is a tendency for fewer super-fibres and loose associations of fibrils and more uniform fibrils observed at $pD\geq11$, with typical dimensions: wide width ~10–11 nm, narrow width ~5–7 nm, twist pitch ~140 nm and length >1 μm. This pH range is above the pK_a of free ornithine, indicating different packing when only the glutamic acid is charged.

Electron micrographs also reveal the presence of rings with d=5–25 nm, thin tapes $w\approx2.5\pm0.5$ and nanoparticles in D_2O and 130 mM NaCl at pD values above 8 and 4, respectively. Rings can most clearly be seen in Figure 4c in which the uranyl acetate stain has collected inside the looped tapes. Each ring appears to be composed of thin tapes 2–3 nm in width.

Peptide P_{11}-9 has the same ionisable side chains (arginine in position 3 and glutamic acid in positions 5, 7 and 9) as P_{11}-4 but the glutamine residues ($-CH_2CH_2CONH_2$) at positions 1, 2, 10 and 11 have been replaced by serine residues ($-CH_2OH$). In this way, whilst retaining the pH responsive behaviour of P_{11}-4 the relative hydrophilicity of the peptide molecule has been increased.

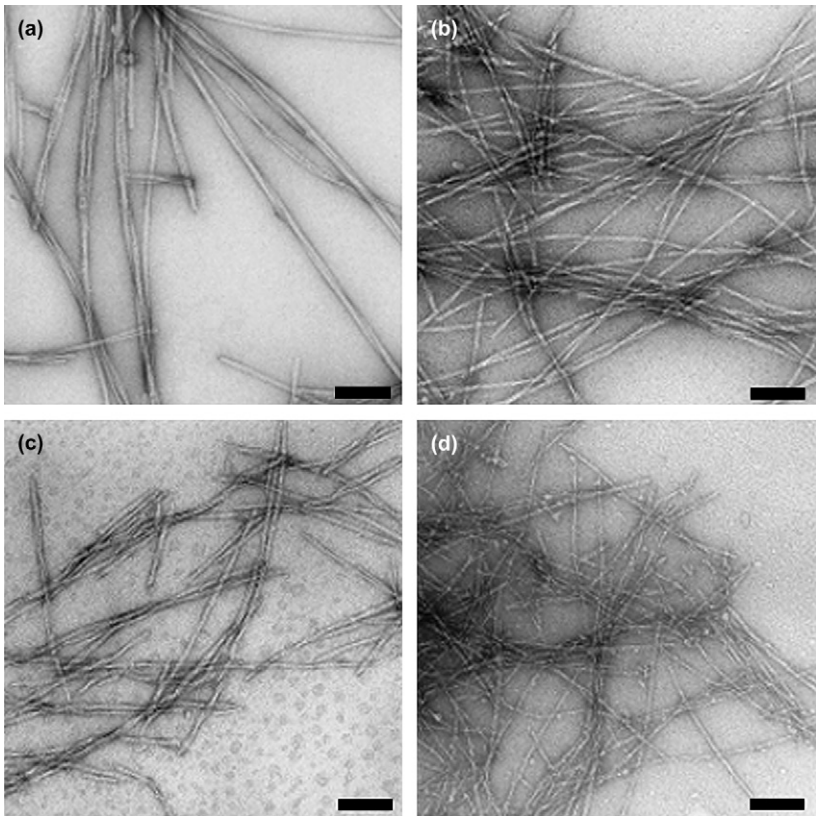

Figure 4. TEM of P_{11}-8 (c=6.4 mM): (a) biphasic solution of nematic gel and isotropic fluid of P_{11}-8 at pD 8.4 in D_2O, (b) a nematic gel of P_{11}-8 at pD 11 in D_2O, (c) a nematic gel of P_{11}-8 at pD 11 in 130 mM NaCl in D_2O, (d) a nematic gel of P_{11}-8 at pD 13.5 in 130 mM NaCl in D_2O. Scale bars 100 nm.

P_{11}-9 (c=7.0 mM) forms clear self-supporting gels at pD$\leq$3.2$\pm$0.2 in D_2O (Fig. 5a). FTIR spectra of the gels (Fig. 5c(i)) have a large absorption band at 1614 cm^{-1} corresponding to β-sheet aggregates and a weaker band at 1684 cm^{-1} indicating an antiparallel β-sheet. In addition, a band at 1710 cm^{-1} corresponding to COOD (protonated glutamic acid side chains) is observed. At 3.2$\leq$pD$\leq$6.8, flocculates are obtained. The percentage of β-sheet within the flocculate is shown to be comparable to that in the self-supporting gels (Fig. 5a), but the fibrillar aggregates are insoluble. At pD$\leq$3.2 the gels have a single positive charge (arginine in position 3). Glutamic acid side chains begin to be deprotonated as the pD is increased, and a situation where the peptide molecules have a net charge of 0 (+1 Arg, −1 Glu) will be encountered. Without sufficient repulsion between the fibrils, large insoluble aggregates are formed leading to flocculation. This explanation is evidenced by the disappearance of the very weak band at 1700 cm^{-1} and the increase in a band at 1565 cm^{-1} which corresponds to COO^- (i.e., deprotonated glutamic acid). At 6.8$\leq$pD$\leq$7.2, clear viscous fluids are obtained as the peptide molecules begin to have a slight net negative charge and the fibrillar aggregates become soluble. At pD>7.2 clear isotropic fluids are observed, accompanied by a characteristic random coil band at 1645 cm^{-1}. The FTIR spectra of viscous fluids at 6.8$\leq$pD$\leq$7.2 can be seen to contain similar proportions of random coil (1645 cm^{-1}) and β-sheet (1614 cm^{-1}).

Addition of salt shifts the conformation transition by more than 3 units to higher pH (Fig. 5b) and makes the transition broader compared to that in the absence of salt. As may be expected, the pH responsive behaviour of P_{11}-9 is similar to that of P_{11}-4. However, P_{11}-9 forms clear self-supporting gels at pD 2 and gives rise to clear nematic fluids or gels at pD 7.5 whereas P_{11}-4 forms cloudy gels or fluids.

The gels of P_{11}-9 at pD$\leq$3 are shown by electron microscopy to be composed of fibrils micrometres in length, which are typically 5–7 nm at their widest point and 4 nm at their narrowest point (Fig. 6). A twist pitch of 50–80 nm is observed. Most fibrils are composed of two thinner structures, 2–4 nm in width. Occasionally fibrils 10 nm in width, composed of three strands 2–3 nm in width each are observed. At this pD value, rings 5–10 nm in width are also observed. Thin tapes, 2–3 nm in width are observed in the background. Flocculates at 3.2$\leq$pD$\leq$6.8 and nematic fluids at 6.8$\leq$pD$\leq$7.2 contain fibrils of the 5–10 nm in width an micrometres in length. These appear to have a slightly less helical appearance. Rings 10 nm in width form by the end to end contact of short aggregates 3–4 nm in width. Tapes 3–4 nm in width are also observed in the background.

Peptide P_{11}-12 has serine residues in positions 1, 2, 10 and 11 similar to P_{11}-9, but is designed through the incorporation of ornithine side chains in positions 5 and 7 to have pH responsive behaviour analogous to P_{11}-8.

Solutions of P_{11}-12 at pD<9 have an absorption band at 1645 cm^{-1} corresponding to peptide in a random coil state. The large absorption band at 1673 cm^{-1} corresponds to TFA^- as observed previously for P_{11}-8 (Fig. 7a). Bands centred at 1614 cm^{-1} and 1625 cm^{-1} were assigned to peptide in

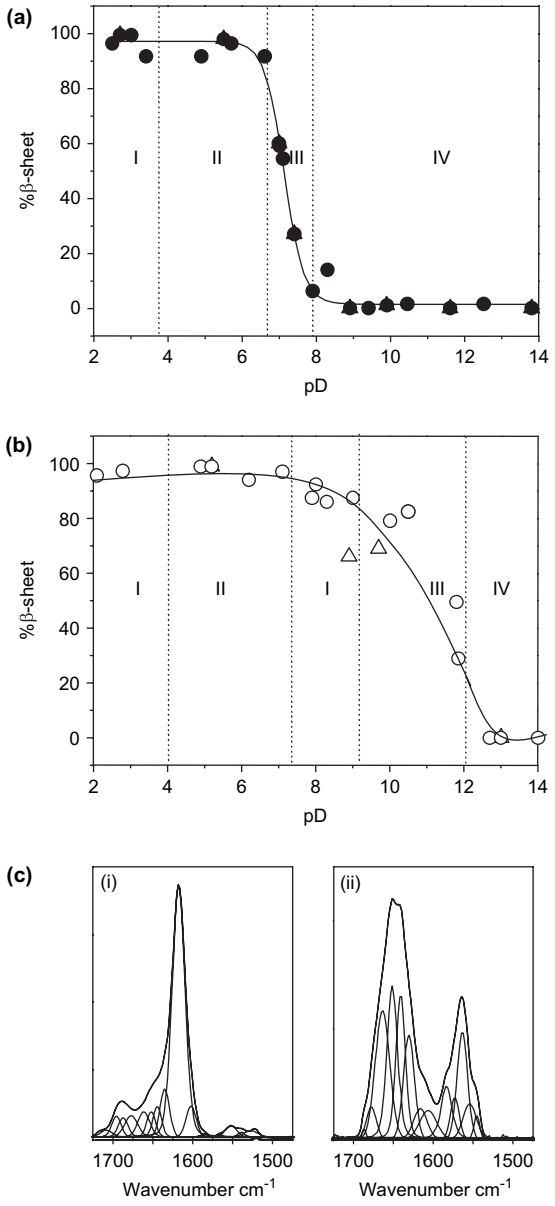

Figure 5. Self-assembly behaviour of P_{11}-9 (c=7.0 mM). (a) Percentage β-sheet of P_{11}-9 as determined by FTIR (●) and NMR (▲) as a function of pD in D_2O. (b) Percentage β-sheet of P_{11}-9 as determined by FTIR (○) and NMR (△) as a function of pD in 130 mM NaCl in D_2O: I: nematic gel, II: flocculate, III: nematic fluid, IV: isotropic fluid. (c) FTIR absorption spectra of P_{11}-9: (i) nematic self-supporting gel at pD 2 in D_2O, (ii) monomeric isotropic fluid at pD 10 in D_2O.

a β-sheet conformation and were seen to increase in magnitude as a function of pD. The weak absorption bands at 1695 cm^{-1} and 1685 cm^{-1} indicate an antiparallel arrangement. At pD<4.4 a weak absorption band centred at 1710 cm^{-1} is observed (assigned to COOD). At pD≥4.4 this band is not observed and a band in the amide II′ region at 1565 cm^{-1} assigned to COO^- is seen. The band at 1565 cm^{-1} increases in intensity as the pD is increased, reflecting the deprotonation of the glutamic acid side chains above their pK_a value (the pK_a of free glutamic acid is 4.25). In the range 9.5<pD<11.5, the amount of β-sheet present is nearly 100%. However at pD>11.5, it starts dropping again. This may be explained by the increased presence of negatively charged carbamates and glutamic acid side chains and the loss of the positive charge on the arginine at pD>12.5, as also discussed for P_{11}-8. This makes the net peptide charge higher than −1 and partially destabilises the aggregates at very high pD. Addition of salt causes the conformation transition to shift by 2 pD units to lower pD (Fig. 7b).

In the absence of added salt at pD≤8 in D_2O, fibrils are not observed. However, at pD 8 a number of 'nanoparticles' and rings are observed 5–40 nm in diameter. At 8.5≤pD≤12, fibrils and bundles composed of 3–4 nm wide fibrils are observed (Fig. 8). These are observed concurrent with nanoparticles 3–25 nm in diameter. Rings ∼5–10 nm in diameter are also observed over the range of pD 2–14, and are formed by ribbons or fibrils 2–3 nm in width. Dark spots formed by the accumulation of uranyl acetate stain within the rings are evident. In solution containing 130 mM NaCl, the transition from nanoparticles to fibrils happens at a different pD value, but the observed morphologies are consistent for each bulk phase. The fibrils formed by P_{11}-12 are very similar to those observed for P_{11}-9, in agreement with the observation made for P_{11}-4 and P_{11}-8 that the peptide sequence dominates behaviour.

Discussion. Our data show that these charged peptide solutions are reminiscent of the behaviour of polyelectrolyte molecules and complexes.[30] Our results are also in-line with data obtained with other gel-forming self-assembling peptide model systems reported in the literature.[2,4,12,31] A class of amphiphilic self-assembling peptides with complementary charges present on each molecule has been previously developed primarily for applications as 3D scaffolds for tissue engineering.[1] Aqueous gels formed by one such peptide (KFE12) at a concentration of 1 wt % have been studied in the presence of different salts (KCl, K_2SO_4 and $K_3Fe(CN)_6$), particularly in terms of their rheological properties. It has been shown that KFE12 undergoes β-sheet self-assembly when the intermolecular electrical double-layer repulsion becomes less than the van der Waals attraction. This is quantified by the DLVO theory, which predicts that addition of salts would screen charged groups from each other and would thus decrease the Debye length of the solvent.[32,33]

A family of peptide amphiphiles consisting of a long hydrocarbon chain segment followed by a peptide segment has also been previously presented. Detailed studies of the rheological properties of aqueous solutions of a typical molecule PA-1 as a function of pH and a wide range of counterions have recently been published.[3] The data show that self-assembly of PA-1 into networks of cylindrical micelles and gelation are triggered by counterion screening, and are in agreement with the DLVO theory. The behaviour of the P_{11} series of peptides presented in this paper is also qualitatively consistent with the DLVO theory, although the effects of different concentrations of salt, or of different types of counterions have not been investigated in detail. The Debye screening length is 0.96 nm in 0.1 M monovalent salt (NaCl) compared with ∼10 nm in the buffered solutions.[34] This order of magnitude change in the screening length shifts the pD for self-assembly by ∼4 points (4 orders of magnitude in deuterium ion concentration, since pD=−log[D^+] by definition). The increased broadening of the range of pD over which self-assembly occurs with the

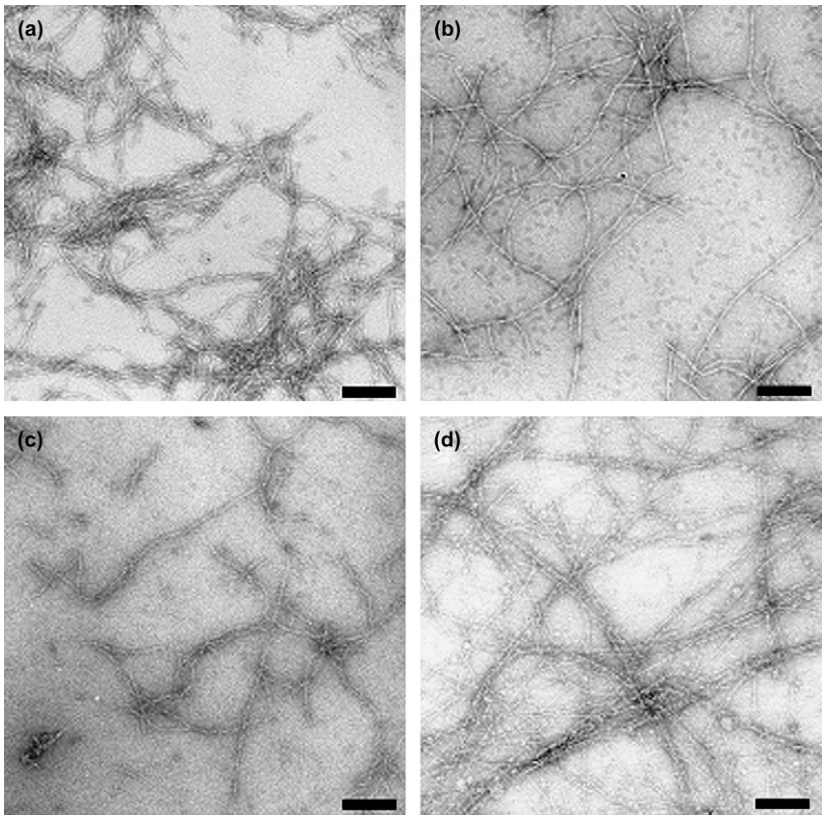

Figure 6. TEM of P_{11}-9 (c=7.0 mM): (a) nematic gel at pD 2 in D_2O, (b) viscous fluid at pD 7 in D_2O, (c) weak gel of P_{11}-9 at pD ~3 in 130 mM NaCl in D_2O, (d) nematic gel at pD ~8 in 130 mM NaCl in D_2O. Scale bars 100 nm.

addition of salt is related to the smaller short range electrostatic forces that cause the break up of fibrils in the fully charged state. These weaker interactions allow a wider range of fibrillar morphologies to coexist at a given value of the pD in high salt conditions, due to the smaller energies that are needed to interconvert between the competing self-assembled structures.

A different class of self-assembling peptides each adopting a hairpin structure has also been designed. The gelation and kinetics of self-assembling hydrogels of the 20 amino acid residue long positively charged MAX1 peptide has been investigated as a function of pH, ionic strength and temperature, using rheology, microrheology and circular dichroism spectroscopy.[5,35] At neutral pH in the absence of salt, the peptide remains monomeric random coil at a concentration of <2 wt %. By raising the ionic strength of the solution the peptide starts forming self-assembling β-sheets and hydrogels, whose mechanical properties increase with increasing salt concentration. These studies demonstrated the importance of ionic strength of the solution for peptide self-assembly and for tuning the mechanical properties of the resulting gels. Self-assembling fibres based on coiled-coil helical peptides have also recently been reported to be stable in physiological-like salt concentrations.[6]

3. Conclusions

Aqueous solutions (10 mg ml^{-1}, equivalent to ~6.3 mM or ~0.7% v/v) of 11 amino acid residue amphiphilic β-sheet tape-forming peptides (P_{11}-4 and P_{11}-9) containing 3 glutamic acid side chains per molecule are found to undergo significant changes as a function of pD (2–14), depending on the deprotonation state of the side chains. Insoluble flocculates of self-assembling fibrils are observed when the net peptide charge is close to zero, nematic gels when there is a small amount of net charge and monomeric fluid when there is a high net charge per peptide (−2 for solutions with no added salt, and −3 for solutions with 130 mM added NaCl).

In the absence of added salt, a sharp transition at 6.5<pD<8 is observed for P_{11}-4 and P_{11}-9 from the antiparallel β-sheet at pD<6.5 to the monomeric random coil at pD>8 as monitored using FTIR and solution ^{1}H NMR. This is accompanied by a change of the solution properties from a nematic solution at pD<8 to isotropic Newtonian fluid at pD>8. The transition is reversible several times by cycling the pD up and down.

In the presence of 130 mM NaCl, the transition becomes broader and shifts to higher pD, by 4 pD units. In addition, at physiological-like conditions (pD ~7–8), self-supporting nematic gels are now obtained. The shift of the transition to higher pD is attributed to screening of electrostatic repulsion between negative charges, rather than to a change in the pK_a of glutamic acid residues in the presence of the added salt.

Aqueous solutions (10 mg ml^{-1}, equivalent to ~7 mM or ~0.7% v/v) of 11 amino acid residue amphiphilic tape-forming peptide variants (P_{11}-8 and P_{11}-12) containing 3 positively charged side chains (one arginine and two

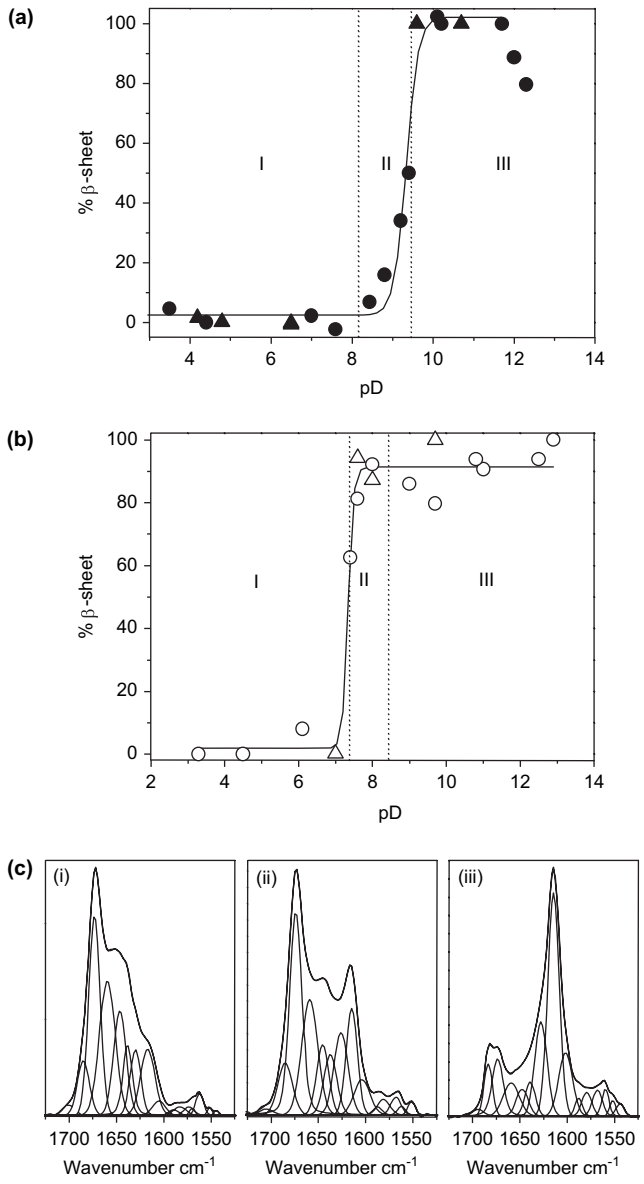

Figure 7. Self-assembly of P_{11}-12 at c=7.1 mM. (a) Percentage β-sheet of P_{11}-12 as determined by FTIR (●) and NMR (▲) as a function of pD in D_2O. (b) Percentage β-sheet of P_{11}-12 as determined by FTIR (○) and NMR (△) as a function of pD in 130 mM NaCl in D_2O: I: isotropic fluid, II: weakly nematic viscous fluid, III: weakly nematic gel. (c) FTIR absorption spectra of P_{11}-12 in D_2O showing (i) monomeric peptide at pD 7, (ii) a viscous fluid at pD 9, (iii) a self-supporting gel at pD 10.

ornithines) per molecule are also found to undergo major changes as a function of pD (2–14), depending on the deprotonation state of the side chains. In the absence of added salt, a transition at 8<pD<10 is observed from gels with antiparallel β-sheet structure at pD>10 to fluid solutions with monomeric random coil peptides at pD<8. In the presence of 130 mM NaCl, the transition shifts to lower pD by 2–3 pD units. In this way, at physiological-like conditions (pD ~7–8), viscous nematic fluids are now obtained, which convert to self-supporting gels at higher peptide concentration.

Careful studies of the morphology of the self-assembling fibrils by TEM revealed a surprising observation, namely that the most frequently observed fibrillar structures for a given peptide appear to be largely independent of ionic strength, phase (i.e., gel, flocculate or nematic solution) and pD. In contrast, the characteristics of the fibrils seem to change significantly by modifications of the peptide primary structure and to a lesser extent by the presence of positively or negatively charged side chains. For example, the most striking difference between P_{11}-4 (− charged) and P_{11}-8 (+ charged variant) fibrils is the tendency for the P_{11}-8 fibrils to be loosely associated allowing the composition of the fibres to be ascertained. P_{11}-4 fibres are more tightly packed, and may in fact be comprised of fewer more highly twisted fibrils.

The insight gained in this study on the self-assembling properties of charged peptides in physiological-like pH and ionic strength, has led to the development of new injectable self-assembling peptide lubricants as potential therapeutics for treatment of early stage knee joint osteoarthritis.[36] A wide range of systematically designed charged peptides have been screened and solutions of P_{11}-9 peptide in physiological buffer have been found to be the most effective in reducing the friction between cartilage plates with small degree of roughness on their surface, mimicking early stage osteoarthritic knee joints.

4. Experimental methods

4.1. Peptide synthesis

Peptides P_{11}-4 and P_{11}-8 were purchased from Neosystem Groupe SNPE (Strasbourg, France) and P_{11}-4, P_{11}-8, P_{11}-11 and P_{11}-12 were also purchased from SynPep (Dublin, USA). All peptides were prepared using standard solid phase Fmoc chemistry.[15] P_{11}-4 and P_{11}-9 were purified by reversed-phase HPLC using 0.1% NH_3 in water as buffer A and 10% buffer A in acetonitrile as buffer B. Peptides P_{11}-8 and P_{11}-12 were purified using a 20–40% water–acetonitrile gradient in the presence of 0.1% TFA. Peptide quality control was carried out using mass spectroscopy, HPLC, amino acid and elemental analysis (carbon, hydrogen, nitrogen and fluorine). Peptide purities were shown to be >93% by HPLC. All peptides were stored at −4 °C as white fluffy powders, produced after freeze-drying. P_{11}-4 (theoretical mass: 1595.7, mass found: 1596, HPLC purity: 96.1%, appearance: white powder); P_{11}-8 (theoretical mass: 1567.2, mass found: 1567.1, HPLC purity: 95.6%, appearance: white powder); P_{11}-9 (theoretical mass: 1431.5, mass found: 1431.5, HPLC purity: 93.1%, appearance: white powder); P_{11}-12 (theoretical mass: 1401.6, mass found: 1401.5, HPLC purity: 95.4%, appearance: white powder).

4.2. TEM

TEM images were collected using a Philips CM 10 TEM at 80 kV accelerating voltage as described previously.[15] The peptide solutions were diluted to a peptide concentration of 20 μM using D_2O adjusted to the appropriate pD, and a drop applied to an ionised, carbon coated copper grid for 60 s. Excess material was removed using filter paper, and a droplet of 4% uranyl acetate was applied to the grid for 20 s. Excess stain was removed, and the grid left to dry on filter paper.

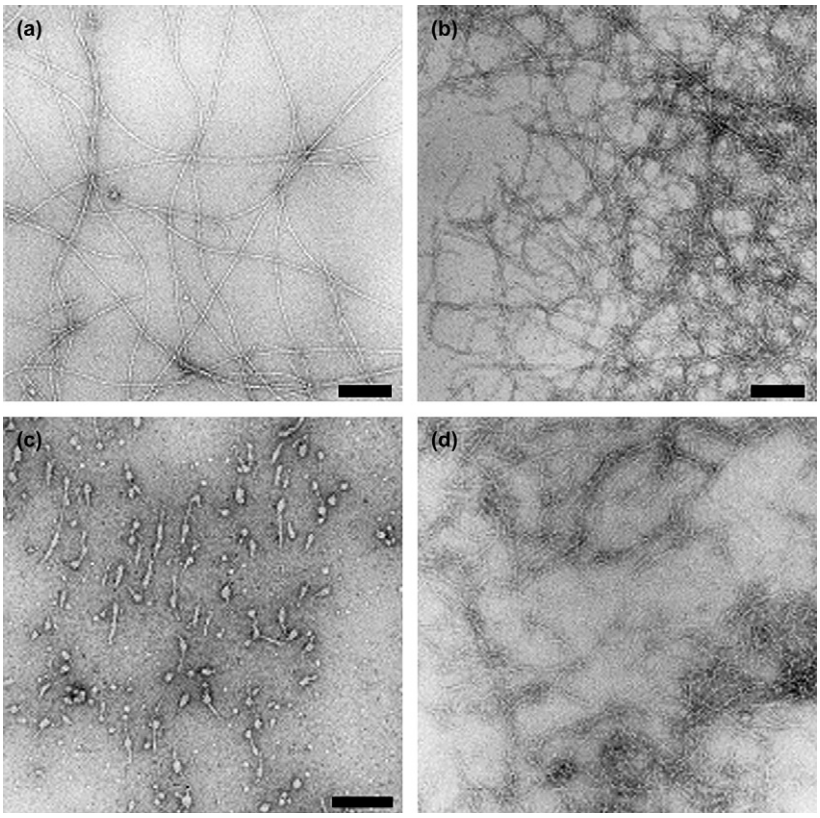

Figure 8. TEM of P_{11}-12 (c=7.1 mM): (a) nematic fluid at pD 8.5 in D_2O, (b) nematic gel at pD 12 in D_2O, (c) isotropic fluid at pD 6 in 130 mM NaCl in D_2O, (d) nematic gel at pD 10 in 130 mM NaCl in D_2O. Scale bars 100 nm.

4.3. FTIR

Spectra were recorded on a Nicolet Avatar 360 FTIR spectrometer. An appropriate volume of D_2O or 130 mM NaCl in D_2O, was added to weighed lyophilised peptide. The pD was then adjusted by the addition of small volumes of DCl or NaOD to produce samples with a range of pD values (pD 1–14) to give a final peptide concentration of 10 mg ml^{-1} (corresponding for P_{11}-4, P_{11}-8, P_{11}-9 and P_{11}-12, to 6.27 mM, 6.38 mM 7.0 mM and 7.1 mM, respectively).

The solutions were left to equilibrate for five days at 20 °C, until no further change was observed in the consistency of the samples. Samples were placed between CaF_2 crystals separated by a 50 μm Teflon spacer. Spectra were averages of 64 scans recorded at room temperature purging with dry air. Blank solvent spectra were subtracted from the sample trace, the baseline corrected and the spectra smoothed. The proportion of peptide in β-sheet aggregates was calculated by the deconvolution of the amide I′ region of the experimental spectra and the determination of the ratio of peptide in β-sheet aggregates to the total (discounting bands not associated with peptide backbone conformation). These values were normalised to the NMR data (see below).

4.4. NMR

^{1}H NMR were carried out using a Bruker DPX 300 MHz instrument. Solutions for NMR were prepared as described previously for IR. For peptide solutions of P_{11}-4 and P_{11}-9, (2,2,3,3-d_4) trimethyl-3 propionic acid, sodium salt (d_4-TMSP) was added to each solution at a concentration of 1 mM as an internal reference. The integral of the area of the aromatic peaks between a set range of parts per million values was calculated. The ratio of the area of the integral of the aromatic peaks to the integral of the control TMSP peak at 0 ppm was determined and normalised between 100% monomer (for the maximum intensity obtained) and 0% monomer (where 0% monomer would correspond to no measurable intensity). However, in P_{11}-8 solutions the TMSP peak at 0 ppm was not observed indicating that the negatively charged molecule was interacting with the (net) positively charged peptide. Therefore, for P_{11}-8 and P_{11}-12 the height of the integral of the aromatic peaks was normalised against the baseline noise.

Acknowledgements

The authors greatly acknowledge the financial support of EPSRC and of the Royal Society. A.A. is a Royal Society University Research Fellow.

References and notes

1. Zhang, S. G.; Holmes, T.; Lockshin, C.; Rich, A. *Proc. Natl. Acad. Sci. U.S.A.* **1993**, *90*, 3334–3338.
2. Mathumura, S.; Uemura, S.; Mihara, H. *Supramol. Chem.* **2006**, *18*, 397–403.
3. Stendahl, J. C.; Rao, M. S.; Guler, M. O.; Stupp, S. I. *Adv. Funct. Mater.* **2006**, *16*, 499–508.

4. Colier, J. H.; Hu, B. H.; Ruberti, J. W.; Xhang, J.; Shum, P.; Thompson, D. H.; Messersmith, P. B. *J. Am. Chem. Soc.* **2001**, *123*, 9463–9464.
5. Ozbas, B.; Kretsinger, J.; Rajagopal, K.; Schneider, J. P.; Pochan, D. J. *Macromolecules* **2004**, *37*, 7331–7337.
6. Smith, A. M.; Banwell, E. F.; Edwards, W. R.; Pandya, M. J.; Woolfson, D. N. *Adv. Funct. Mater.* **2006**, *16*, 1022–1030.
7. Reches, M.; Gazit, E. *Nat. Nanotechnol.* **2006**, *1*, 195–200.
8. Smith, J. F.; Knowles, T. P. J.; Dobson, C. M.; MacPhee, C. E.; Welland, M. E. *Proc. Natl. Acad. Sci. U.S.A.* **2006**, *103*, 15806–15811.
9. Rogers, S. S.; Venema, P.; Sagis, L. M. C.; van der Linden, E.; Donald, A. M. *Macromolecules* **2005**, *7*, 2948–2958.
10. de la Paz, M. L.; Goldie, K.; Zurdo, J.; Lacroix, E.; Dobson, C. M.; Hoenger, A.; Serrano, L. *Proc. Natl. Acad. Sci. U.S.A.* **2002**, *99*, 16052–16057.
11. Hartgerink, J. D.; Beniash, E.; Stupp, S. I. *Science* **2001**, *294*, 1684–1688.
12. Mart, R. J.; Osborne, R. D.; Stevens, M. M.; Ulijn, R. V. *Soft Matter* **2006**, *2*, 822–835.
13. Aggeli, A.; Bell, M.; Boden, N.; Keen, J. N.; Knowles, P. F.; McLeish, T. C. B.; Pitkeathly, M.; Radford, S. E. *Nature* **1997**, *386*, 259–262.
14. *Self-Assembling Peptide Systems in Biology, Medicine and Engineering*; Aggeli, A., Boden, N., Zhang, S., Eds.; Kluwer Academic: The Netherlands, 2001.
15. Aggeli, A.; Bell, M.; Boden, N.; Keen, J. N.; McLeish, T. C. B.; Nyrkova, I. A.; Radford, S. E.; Semenov, A. N. *J. Mater. Chem.* **1997**, *7*, 1135–1145.
16. Aggeli, A.; Boden, N.; Fytas, G.; McLeish, T. C. B.; Mawer, P.; Vlassopoulos, D. *Biomacromolecules* **2001**, *2*, 378–388.
17. Carrick, L.; Tassieri, M.; Waigh, T. A.; Aggeli, A.; Boden, N.; Bell, C.; Fisher, J.; Ingham, E.; Evans, R. *Langmuir* **2005**, *21*, 3733–3737.
18. Kayser, V.; Turton, D.; Aggeli, A.; Beevers, A.; Reid, G. D.; Beddard, G. *J. Am. Chem. Soc.* **2004**, *126*, 336–343.
19. Davies, R. P. W.; Aggeli, A.; Beevers, A. J.; Boden, N.; Carrick, L. M.; Fishwick, C. W. G.; McLeish, T. C. B.; Nyrkova, I.; Semenov, A. N. *Supramol. Chem.* **2006**, *18*, 435–443.
20. Aggeli, A.; Nyrkova, I. A.; Bell, M.; Harding, R.; Carrick, L.; McLeish, T. C. B.; Semenov, A. N.; Boden, N. *Proc. Natl. Acad. Sci. U.S.A.* **2001**, *98*, 11857–11862.
21. Nyrkova, I. A.; Semenov, A. N.; Aggeli, A.; Boden, N. *Eur. Phys. J. B* **2000**, *17*, 481–497.
22. Nyrkova, I. A.; Semenov, A. N.; Aggeli, A.; Bell, M. P.; Boden, N.; McLeish, T. C. B. *Eur. Phys. J. B* **2000**, *17*, 499–513.
23. Fishwick, C. W. G.; Beevers, A.; Carrick, L.; Whitehouse, C.; Aggeli, A.; Boden, N. *Nano Lett.* **2003**, *3*, 1475–1479.
24. Meegan, J.; Aggeli, A.; Boden, N.; Brydson, R.; Brown, A.; Carrick, L. M.; Brough, A.; Hussain, A.; Ansell, R. J. *Adv. Funct. Mater.* **2004**, *14*, 31–37.
25. Firth, A.; Aggeli, A.; Burke, J. L.; Yang, X.; Kirkham, J. *Nanomedicine* **2006**, *1*, 189–199.
26. Whitehouse, C.; Fang, J.; Aggeli, A.; Bell, M.; Brydson, R.; Fishwick, C. W. G.; Henderson, J.; Knobler, C. M.; Owens, R. W.; Thomson, N. H.; Smith, D. A.; Boden, N. *Angew. Chem., Int. Ed.* **2005**, *44*, 1965–1968.
27. Aggeli, A.; Bell, M.; Carrick, L.; Fishwick, C. W. G.; Harding, R.; Mawer, P.; Radford, S. E.; Strong, A.; Boden, N. *J. Am. Chem. Soc.* **2003**, *125*, 9619–9628.
28. Aggeli, A.; Bell, M.; Boden, N.; Carrick, L. M.; Strong, A. *Angew. Chem., Int. Ed.* **2003**, *42*, 5603–5606.
29. Edsall, J. T.; Gutfreund, H. *Biothermodynamics: The Study of Biochemical Processes at Equilibrium*; John Wiley and Sons: Chichester, UK, 1983; Chapter 5, pp 157–209.
30. Tsuchida, E.; Abe, K. *Adv. Polym. Sci.* **1982**, *45*, 1–119.
31. Collier, J. H.; Messersmith, P. B. *Bioconjugate Chem.* **2003**, *14*, 748–755.
32. Caplan, M. R.; Moore, P. N.; Zhang, S. G.; Kamm, R. D.; Lauffenburger, D. A. *Biomacromolecules* **2000**, *1*, 627–631.
33. Caplan, M. R.; Schwartzfarb, E. M.; Zhang, S. G.; Kamm, R. D.; Lauffenburger, D. A. *Biomaterials* **2002**, *23*, 219–227.
34. Israelachvili, J. *Intermolecular and Surface Forces*, 2nd ed.; Academic: London, 1991.
35. Veerman, C.; Rajagopal, K.; Palla, C. S.; Pochan, D. J.; Schneider, J. P.; Furst, E. M. *Macromolecules* **2006**, *39*, 6608–6614.
36. Bell, C. J.; Carrick, L. M.; Jin, Z. M.; Ingham, E.; Aggeli, A.; Boden, N.; Waigh, T. A.; Fisher, J. *J. Biomed. Mater. Res. A* **2006**, *78A*, 236–246.